

Statistical Analysis of Asteroids

Nam Nguyen, Qian Chen, Feni Pandya, Willie Lo

December 9, 2019

Contents

1	Introduction	3
1.1	Objective	3
1.2	Datasets	3
2	Asteroids	3
2.1	Background	3
2.2	Orbital Parameters	4
2.3	Types of Asteroids	5
2.4	Correlation Matrix	5
2.5	Temperature	6
2.6	Delta-V	7
2.7	Potentially Hazardous Asteroids	8
2.8	Asteroid Classification	9
3	Exoplanets	11
3.1	Background	11
3.2	Discovery Methods	11
3.3	Analysis	12
4	Future Scope	13
4.1	Saturn's Rings	13
4.2	Future Impacts	14
4.3	Exoplanet Discoveries	14
5	References	14

1 Introduction

1.1 Objective

Our main goal was to try to confirm existing physical formulas and theories and potentially identify trends that are not yet explained by current theories.

1.2 Datasets

Our primary dataset is the JPL Small Body Database, which was downloaded from the publicly available search engine of the same name. It is currently the most comprehensive database on small objects in our Solar System to date, and is maintained and updated on a daily basis by NASA's Jet Propulsion Laboratory. The dataset contains both physical and orbital parameters of over 800,000 objects, most of which are asteroids. Physical parameters are an object's size, mass, shape, etc. while orbital parameters are related to the object's motion around the Sun.

Our secondary datasets include:

1. Exoplanets from the NASA Exoplanet Archive. The most comprehensive database on discovered exoplanets to date, this dataset contains the physical and orbital parameters of over 4,000 exoplanets along with physical parameters for each planet's parent star. This dataset is of interest because the detection of both exoplanets and asteroids have skyrocketed in recent decades, and both types of objects should theoretically behave in similar ways in space due to gravity, as asteroids are merely miniature planets that did not have enough material to fully form.
2. Near Earth Asteroids (NEA) from the IAU's Minor Planet Center. The three types NEAs we focused on were Apollo, Amor, and Aten asteroids, which are categorized by their slightly different orbital paths around the Earth. These particular asteroids are of interest because there is potential for humans to interact with these asteroids given sufficient technological developments. There is also potential for these asteroids to impact the Earth in the future, in which case they are labeled as Potentially Hazardous Asteroids (PHA).

2 Asteroids

2.1 Background

Asteroids are small, rocky bodies that orbit the Sun in our Solar System. They are theorized to have formed from the materials that remained after the formation of the planets and their natural satellites (i.e. moons). Although both asteroids and comets are made up of rocky materials, the main difference between the two is that asteroids are also composed of metals, whereas comets are composed of ices. By definition, comets are further away from the Sun than asteroids are, as the ices cannot remain frozen in close solar proximity.

Although asteroids are generally scattered throughout space, most of the asteroids in our Solar System are found in the Asteroid Belt between Mars and Jupiter (Figure 1), separating the inner rocky planets from the outer gas giants. Asteroids may also form groups outside of the Asteroid Belt, such as the Jupiter Trojans (Figure 2).

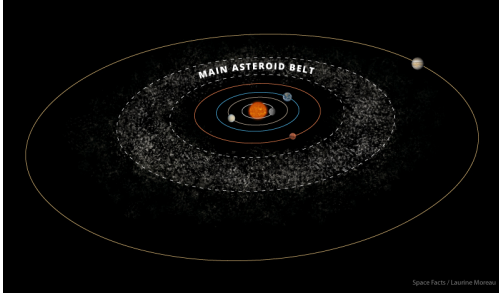


Figure 1: Main Asteroid belt

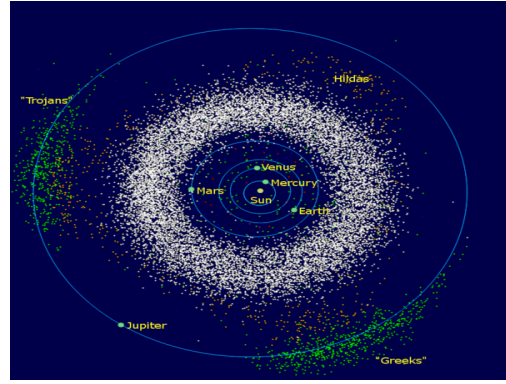


Figure 2: Asteroid belt and Jupiter's Trojans

2.2 Orbital Parameters

Here we provide a description of all of the orbital parameters relevant to our project. Objects in space will orbit a parent object (in our case the parent object is the Sun) in elliptical orbits, where the parent object is at a focus. Note that all angles described are with respect to the Sun, where 0 degrees is the angle between the Earth and the Sun on the Vernal Equinox. Orbital plane angles are relative to the solar ecliptic, which is the plane of the Sun's equator. The distance metric used in astronomy is 1 au = average distance from the Earth to the Sun = 1.496×10^{11} meters.

Parameter	Description
e	eccentricity; circularity of an orbit
a	semi-major axis (au); average distance from the Sun
q	perihelion (au); shortest distance from the Sun
i	inclination (deg); orbital tilt with respect to the solar ecliptic
om	longitude of the ascending node (deg); angle at the point when the asteroid traverses from below to above the ecliptic plane
w	argument of perihelion (deg); angle at perihelion
ma	mean anomaly (deg); a calculated parameter that increases linearly with time
ad	aphelion (au); furthest distance from the Sun
n	mean motion (deg/day); motion averaged across the entire orbit
tp	time of perihelion passage (TDB); the last date that the asteroid was at perihelion
tp _{cal}	time of perihelion passage (ET); perihelion passage in calendar dates
per	sidereal orbital period (days); how long it takes to complete one full orbit
per _y	sidereal orbital period (years); orbital period in years
moid	Earth Minimum Orbit Intersection Distance (au); the closest distance an asteroid is to Earth's orbit
moid _{ld}	Earth Minimum Orbit Intersection Distance (LD); MOID measured in lunar distances
moid _{jup}	Jupiter Minimum Orbit Intersection Distance (au); the closest distance an asteroid is to Jupiter's orbit
t _{jup}	Jupiter Tisserand Invariant; theoretical parameter that distinguishes different types of orbits

Table 1: Orbital Parameters

2.3 Types of Asteroids

Here we list the many groups of asteroids that exist in our Solar System. Asteroid groups are defined by their orbital parameters. In our project, we focus on groups that either have significantly more data available or are relevant to the future of Earth interactions (denoted by an asterisk).

Acronym	Description
IMB*	Inner Main Belt Asteroid
MBA*	Main Belt Asteroid
OMB*	Outer Main Belt Asteroid
MCA*	Mars-Crossing Asteroid
AMO*	Amor Asteroid
APO*	Apollo Asteroid
ATE*	Aten Asteroid
TJN*	Jupiter Trojan
TNO	Trans-Neptunian Object
PAA	Parabolic Asteroid
HYA	Hyperbolic Asteroid
IEO	Interior Earth Object
CEN	Centaur Orbit between Jupiter and Neptune
AST	Asteroid orbit not matching defined orbit classes

Table 2: Asteroid Types

2.4 Correlation Matrix

As a preliminary survey, we created correlation matrices to see how different orbital parameters relate to each other.

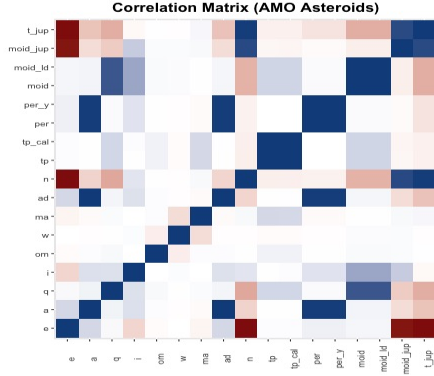


Figure 3: Correlation matrix for Amor asteroids

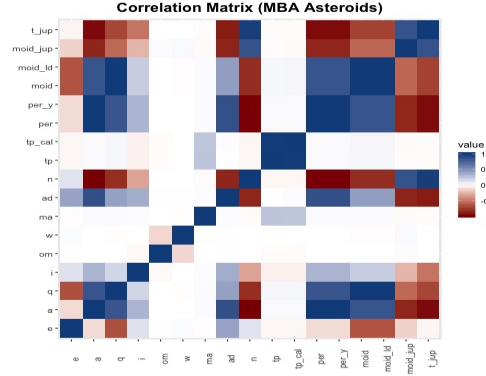


Figure 4: Correlation matrix for main belt asteroids

From Figure 3, we can see a few trends that are readily explained by physics. Period is positively correlated with semi-major axis, which is consistent with Kepler's 3rd Law: $P^2 = a^3$.

However, notice that there are major differences in correlations when comparing the matrices of different asteroid groups. Different groups encompass different orbital shapes, which will affect how their parameters correlate with each other. For example: Earth MOID is not very correlated with eccentricity for Amor asteroids because Amors are already defined to cross Earth's path. However, that same relationship is highly negatively correlated for Main Belt Asteroids because the Asteroid Belt is far away from Earth (1 au) so MBAs have a harder time reaching Earth unless they have highly elliptical orbits. In other words, as eccentricity increases and an MBA orbit becomes more elliptical, its minimum distance from Earth decreases, thus resulting in a negative correlation.

2.5 Temperature

Our first calculation involved finding the surface temperature of each asteroid. As solar radiation reaches an asteroid, the radiation can either be absorbed or reflected. Radiation that is absorbed will be re-radiated as heat, thus increasing the asteroid's temperature. A simple assumption is that the closer an asteroid is to the Sun, the hotter it will be because it will have more radiation to absorb. However, if an asteroid were to be able to reflect a large portion of that radiation, then it would be no hotter than a far away asteroid that absorbs all the radiation it receives. Thus, the albedo, or reflectivity, of an asteroid also plays a role in its temperature.

The total incident power is given by

$$R_{in} = \frac{(1-A)L_0\pi r^2}{4\pi a^2}$$

where A is the albedo, a is the semi-major axis, r is the radius and L_0 is the luminosity of the Sun ($L_0 \approx 3.827 \times 10^{26} W$)

The radiated power from the asteroid is given by

$$R_{out} = 4\pi r^2 \epsilon \sigma T^4$$

where σ is the Stefan-Boltzmann constant ($\sigma \approx 5.6704 \times 10^{-8} W/m^2 K^4$), T is the temperature in kelvins, and ϵ is the asteroid's infra-red emissivity.

We assume that the total incident power is equal to the radiated power at equilibrium. Hence, the surface temperature of the asteroid is as follow

$$T = \left[\frac{(1-A)L_0}{\epsilon \sigma 16\pi a^2} \right]^{1/4}$$

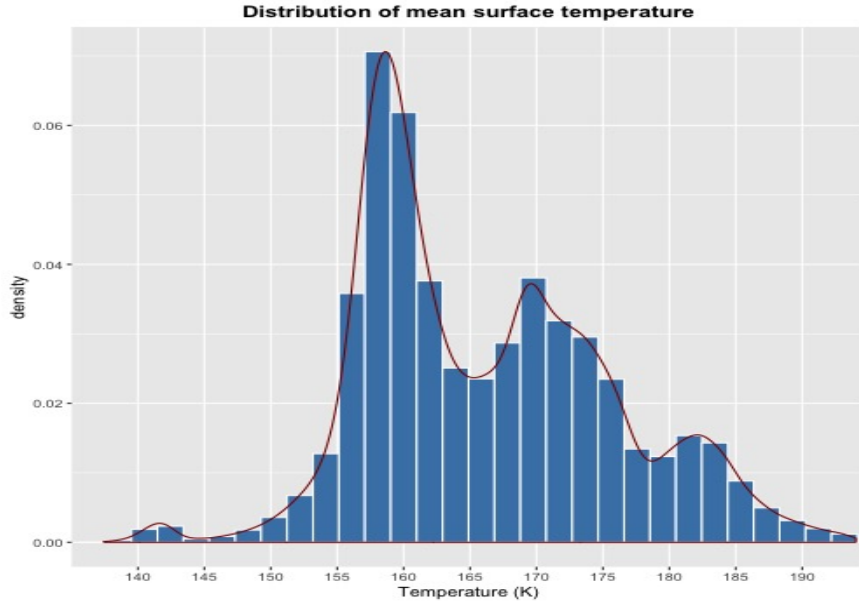


Figure 5: Distribution of mean surface temperature

Immediately, we can identify three major peaks in the asteroid temperature distribution at $\approx 158 K$, $170 K$, and $182 K$. Our hypothesis is that each major peak represents a section of the Asteroid Belt, with $182 K$ representing the inner belt and $158 K$ representing the outer belt. However, this interpretation does not explain why the $158 K$ outer belt peak dominates over the other two peaks, which are expected to be greater

due to the inner and main belt's closer proximity to Earth and their generally greater number density (see Section 2.8: Asteroid Classification). A further study into how asteroid albedo density varies with distance may shed light onto why these peaks do not match real-life expectations. On another note, we see a small bump centered 142 K, which may correspond to the Jupiter Trojans, which are considerably farther away from Earth than Main Belt Asteroids are.

2.6 Delta-V

Delta-V (ΔV) is a measure of the specific impulse required to perform any in-space maneuver. Regarding asteroids, the ΔV metric takes into account an asteroid's velocity and closest approach to Earth to evaluate how much energy is required to rendezvous with said asteroid. As an asteroid's velocity increases, the harder it will be to meet up with it; similarly, the farther away an asteroid is from Earth, the more energy will be required to reach it. In general, the smaller ΔV is for an asteroid, the less energy is required to rendezvous with it and thus the more accessible the asteroid is to us from Earth. This parameter is very important for future endeavors such as asteroid mining and research that would require spacecraft to land on or enter orbit with Near Earth Asteroids.

We calculated the ΔV for three types of Near Earth Asteroids (Figure 7):

1. Amor asteroids, which have perihelia close to but greater than Earth's aphelion so they do not cross Earth's orbit; instead, they form an "outer ring" surrounding Earth. Most of them cross paths with Mars.
2. Apollo asteroids, which are NEAs whose semimajor axes are greater than 1 au but perihelia distances are less than Earth's aphelion distance; these are Earth-crossing asteroids.
3. Aten asteroids, which are almost the opposite of Apollo asteroids in that they are NEAs with semimajor axes less than 1 au but aphelia greater than Earth's perihelion. They are also Earth-crossing, but they only cross Earth when Earth is near perihelion.

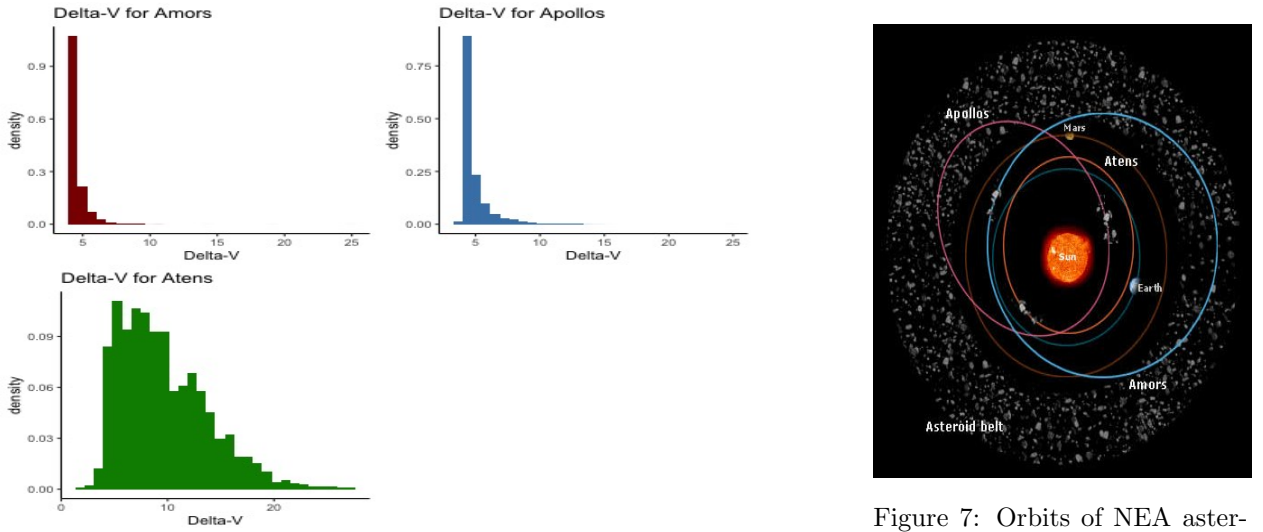


Figure 6: Distribution of ΔV by asteroid types

Figure 7: Orbits of NEA asteroids

The ΔV results are quite puzzling. Amors and Apollos produce very thin distributions peaking around 5, while the Atens distribution is very spread-out. To our knowledge, Amors should require the largest ΔV as their orbits are the largest and their average distances away from the Earth are larger than those of the Apollos and Atens. In fact, we would expect Atens to have the lowest values for ΔV as their orbits are closely subscribed to the Earth's. This discrepancy in expected results could become a topic for future analysis.

2.7 Potentially Hazardous Asteroids

A potentially hazardous object is a near-Earth object with an orbit that can make close approaches to the Earth and large enough to cause significant regional damage in the event of impact. Most of these objects are potentially hazardous asteroids (PHAs), and a few are comets. As of October 2019, there are 2,018 known PHAs (about 10% of the total near-Earth population), of which 156 are estimated to be larger than one kilometer in diameter. Most of the discovered PHAs are Apollo asteroids (1,601) and fewer belong to the group of Aten asteroids (169).

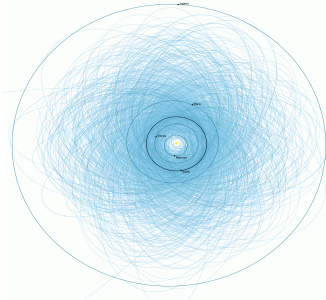


Figure 8: Orbits of over 1,400 known PHAs by the Jet Propulsion Lab at NASA



Figure 9: Radar image of the Toutatis asteroid by GSFC in 1996

In this section, the aim is to predict if an asteroid is hazardous based on its absolute magnitude (the luminosity of a celestial object) and its minimum orbital intersection distance with the Earth. Again, due to computational limitation, we subset the full data set randomly to obtain a training set (20,000 observations) and a test set (30,000 observations). We train the following classification models:

- Support Vector Machine (SVM)
- K-Nearest Neighbors (KNN)
- Logistic Regression

We then apply the models on the test data set to get the out-of-sample performance. Since the data set is highly imbalanced, it makes sense to determine the significance of the models relative to the all-in strategy (labelling everything as non-hazardous). To do this, we use the McNemar's test.

Algorithm	Out-of-sample (%)
SVM	99.733
KNN	99.810
Logit	99.883
All-in	99.733

Table 3: Predictive accuracy of algorithms for PHA

Since the data is very imbalanced (most asteroids are non-hazardous), the all-in strategy yields an accuracy of 99.733% on the test set (this should be the baseline to evaluate other models). Logistic regression is the best method in this case with an out-of-sample accuracy of 99.883%.

Is the logistic regression model significantly better? To answer this question, we use the McNemar's test. The test statistic follows a χ^2 distribution with 1 degree of freedom.

- Logit / All-in: $\chi^2 = 65$, p-value = 7.5×10^{-16}

We conclude that the logistic regression model outperforms the all-in strategy (at reasonable significance level).

2.8 Asteroid Classification

From the exploratory data analysis, we see that orbits of different types show distinct characteristics. To investigate this problem further, we employ machine learning algorithms to predict orbit classification based on eccentricity and semi-major axis.

Due to computational limitations, we cannot work with the entire data set (more than 800,000 asteroids). Instead, we train the models on a random subset of the data. The smallest subset has 1,400 observations and the largest has 14,000 observations. To test the out-of-sample performance of the models, we also extract a test sample with 13,000 observations. The algorithms to be considered are:

- Support Vector Machine (SVM)
- K-Nearest Neighbors (KNN)
- Linear Discriminant Analysis (LDA)
- Quadratic Discriminant Analysis (QDA)
- Generalized Logistic Regression (GLR)

Once the models have been trained, we plot the decision boundaries for each model. It is expected that LDA and Logistic Regression should display linear boundaries whereas decision boundaries for SVM and KNN can be highly non-linear. To do this conveniently, we make a Shiny app, where the user can select the sample size (from 200 to 2,000) and the algorithm to be used. We then compute and compare the predictive accuracy of the models. The models are statistically compared using the Stuart-Maxwell test, which is a generalization of the McNemar's test for multi-class supervised learning problems.

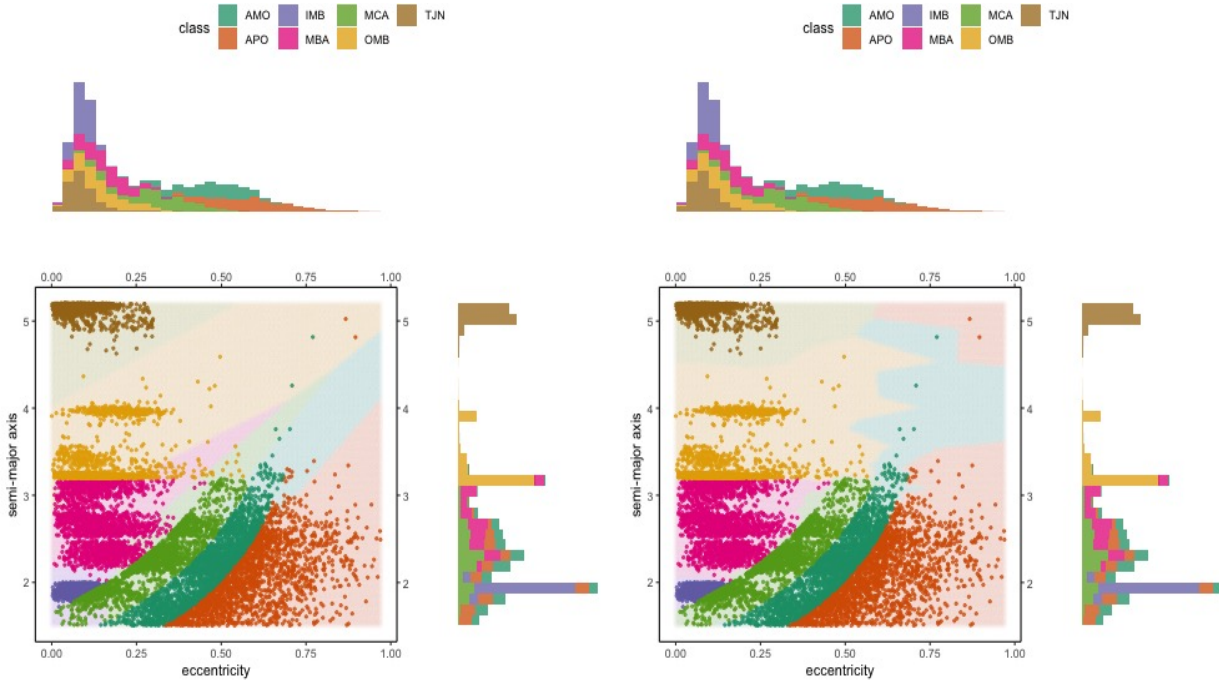


Figure 10: LDA Classification of Orbital Types

Figure 11: KNN Classification of Orbital Types

From Figure 10 and Figure 11, we can see that the decision boundaries for LDA is linear as expected. On the other hand, the boundaries for KNN is much more flexible because it is a non-parametric algorithm.

There are quite a number of trends to be identified with this plot.

1. APO & AMO: For these NEAs, we can see that as eccentricity tends to 1 and the orbit becomes more elliptical, the semi-major axis increases. This is understandable because as an asteroid goes farther away from the Earth, the orbit needs to become more elliptical for the asteroid to maintain contact with the Earth to be classified as a NEA.
2. IMB: This references the inner-most layer of the Asteroid Belt, closest to Mars. The plot shows that IMBs have fairly circular orbits at an average distance of 2 au away from the Sun. This observation is consistent with where the Asteroid Belt begins, around 2.06 au. Highly elliptical orbits would not survive in the Inner Asteroid Belt, as collisions and gravitational effects of other asteroids would cause asteroids with elliptical orbits to be kicked out of the belt.
3. MBA: The middle section of the Asteroid Belt. Because this section is broader and thus more spacious, MBAs can have slightly higher elliptical orbits relative to IMBs without being kicked out of the belt.
4. OMB: The outer layer of the Asteroid Belt. Interestingly, there seem to be two major groups within this region, which can potentially allude to imperfect learning and categorizing by our trained machine. Otherwise, this is an interesting find that may warrant further investigation.
5. MCA: Notice that the Mars-Crossing Asteroids seem to overlap with IMB and MBA. This is because the asteroid belt is right next to Mars. MCAs follow the same trend as NEAs in that larger semi-major axes require higher eccentricity to be within the vicinity of Mars.
6. TJN: The Jupiter Trojans are all clustered around 5 au, which is consistent with Jupiter's distance from the Sun.

The eccentricity histogram above the scatter plot shows that asteroids tend to have more circular orbits than elliptical ones. This could be due to observational bias, as highly elliptical orbits are harder to track and identify due to their variable travel speeds and often-times large semi-major axes. Another explanation could be that most highly elliptical asteroids were kicked out of the Solar System at some point due to their unstable orbits, thereby leaving only the stable, circular orbit asteroids in our Solar System.

From the semi-major axis histogram to the right of the scatter plot, we can see three distinct peaks at around 2 au, 3 au, and 5 au. The peak at 2 au suggests the beginning of the Asteroid Belt, where asteroid density first begins to rapidly increase, and the peak at 5 au corresponds to the Jupiter Trojans. However, the peak at 3 au remains a mystery. We would expect the distribution to either decrease uniformly or remain constant after the initial start of the Asteroid Belt, but instead we see a spike at 3 au, which cannot be linked to any known phenomena or structures within the Asteroid Belt. This is an interesting find that could lead to future discoveries about Asteroid Belt densities.

Algorithm	In-sample (%)	Out-of-sample (%)
SVM	95.312	86.732
KNN	100	95.527
LDA	91.312	73.973
QDA	94.531	85.036
GLR	96.031	88.384

Table 4: Performance of classifiers (n=200)

Algorithm	In-sample (%)	Out-of-sample (%)
SVM	97.293	97.046
KNN	100	98.854
LDA	85.664	85.246
QDA	92.414	92.346
GLR	93.857	94.286

Table 5: Performance of classifiers (n=2,000)

KNN produces the best performance, followed closely by SVM and GLR. LDA has the lowest predictive accuracy on both the test set and the training set. This is expected because LDA assumes linear decision boundaries, which clearly do not hold for this particular problem. We can tune the KNN model (by finding the optimal number of nearest neighbors and the best distance metric) to achieve a better result.

We compare the two best models statistically using the Stuart-Maxwell test. The test statistic follows a χ^2 distribution with $K - 1$ degrees of freedom, where K is the number of classes (i.e. df = 6 in this case).

- n = 1,400, KNN / GLR: $\chi^2 = 374.81$, p-value $\downarrow 2.2 \times 10^{-16}$

- $n = 14,000$, SVM / KNN: $\chi^2 = 276.03$, p-value $< 2.2 \times 10^{-16}$

We conclude that KNN is the best model for this problem.

3 Exoplanets

3.1 Background

We now move our discussion to exoplanets, which are in some ways very similar to asteroids. Just like our Solar System hosts the eight planets (Mercury, Venus, Earth, Mars, Jupiter, Saturn, Uranus, Neptune), other stars within the Milky Way Galaxy and other galaxies can host their own set of planets, which we call exoplanets. Exoplanet data is particularly useful for trying to find relationships between asteroids and planets. While there is surely a correlation in how the Sun's gravity and solar activity affects both the planets and asteroids in our Solar System, there are only eight planets for us to gather data from, whereas with exoplanet data we now have many more planet-star relationships to utilize to produce more robust results. Unfortunately, these analyses were beyond the scope of this project and would better suit one's PhD thesis. However, we are still able to perform preliminary analyses related to asteroid and exoplanet data collection so that such pursuits may be emboldened in the future (See Chapter 4: Future Scope).

3.2 Discovery Methods

There are dozens of methods that are used to discover celestial objects, and only a few of them are effective in discovering exoplanets, which are only as bright as the light they reflect off of their parent star (in other words, they are very very dim and hard to see). Here we denote the five most common exoplanet observational methods used by researchers and see whether they produce the results that are expected of them.

1. Radial Velocity: Because gravity is an attractive force, not only is a planet kept in orbit by the gravitational pull of its parent star, but the star is being pulled by the planet's gravity as well. The star's movement from this interaction is very minimal due to its significantly larger mass compared to that of the planet, but measuring how the star's brightness varies as it is being pulled back and forth by the planet's orbit can produce information about the orbiting planet. This is known as radial velocity because astronomers can use the periodic variations in stellar brightness to calculate the velocity of the star's movements relative to the Earth.

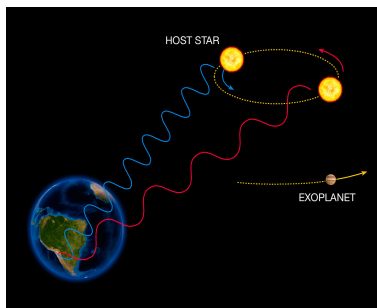


Figure 12: Radial Velocity

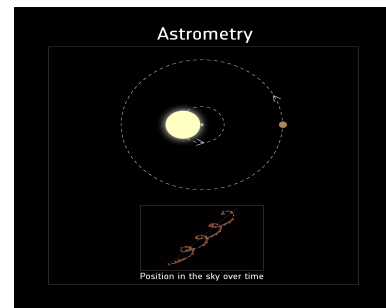


Figure 13: Astrometry

2. Astrometry: This method draws from the same law of gravitation that makes radial velocity calculations possible. However, rather than look at a star's brightness, astronomers look at a star's physical position in space and how it changes in time to perform astrometry calculations.
3. Gravitational Microlensing: Einstein's theory of General Relativity predicted that gravity has the ability to bend light rays. When a parent star or planet passes in front of another star (a source star), the gravity from the transiting object will bend the light rays of that source star, causing the image

of the source star, as seen from Earth, to be warped. Analyzing the differences between the warped, microlensed image and the original image gives astronomers information about the transiting object that bent the light rays.

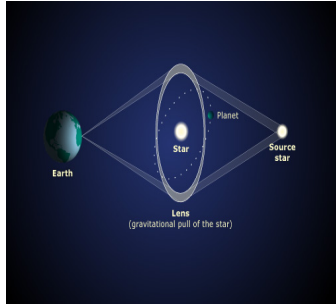


Figure 14: G-Microlensing

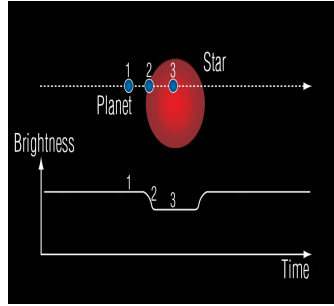


Figure 15: Transit Photometry

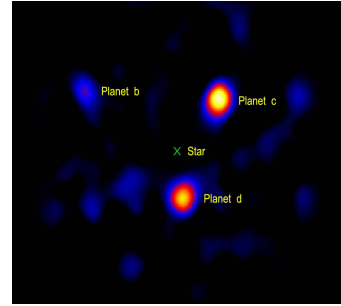


Figure 16: Transit Photometry

4. Transit Photometry: When a planet transits its parent star, part of the star's light is blocked out, making the star appear dimmer than usual. Seeing starlight dim periodically is a good indicator that a planet is orbiting the star.
5. Direct Imaging: This method involves using a telescope or camera to see the planet directly, as opposed to seeing its affect on its parent star. This is one of the harder methods to use to discover planets because planets are very dim compared to the stars around it.

3.3 Analysis

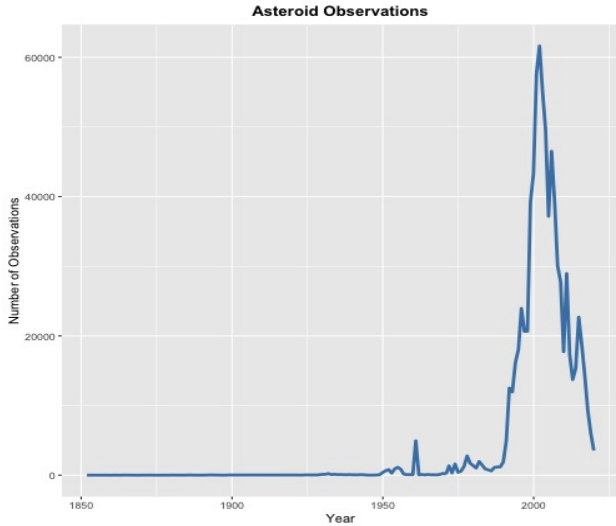


Figure 17: Discovery of asteroids by year

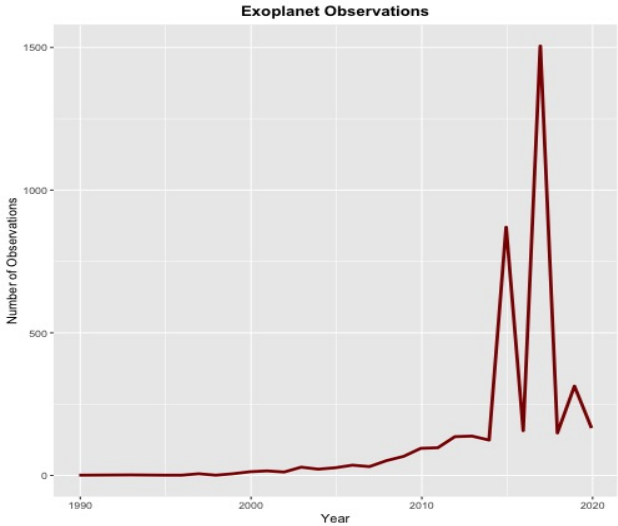


Figure 18: Discovery of exoplanets by year

From the plots above, we can see that asteroid observations began increasing drastically around the 1990s and peaked in the early 2000s. Although we were unable to procure data on specific observational methods for asteroids, we do know that around that time period the scientific community became increasingly concerned with Earth-asteroid collisions due to various discoveries involving the hypothesis that an asteroid caused the mass extinction of the dinosaurs. This concern may have spurred the development of asteroid-detecting technology. In later years, we see that exoplanet observations also begin to skyrocket. The technology used

to detect asteroids undoubtedly spurred the detection of exoplanets beginning also in the 1990s and peaking within the past decade in 2017 due to the development of additional exoplanet technologies.

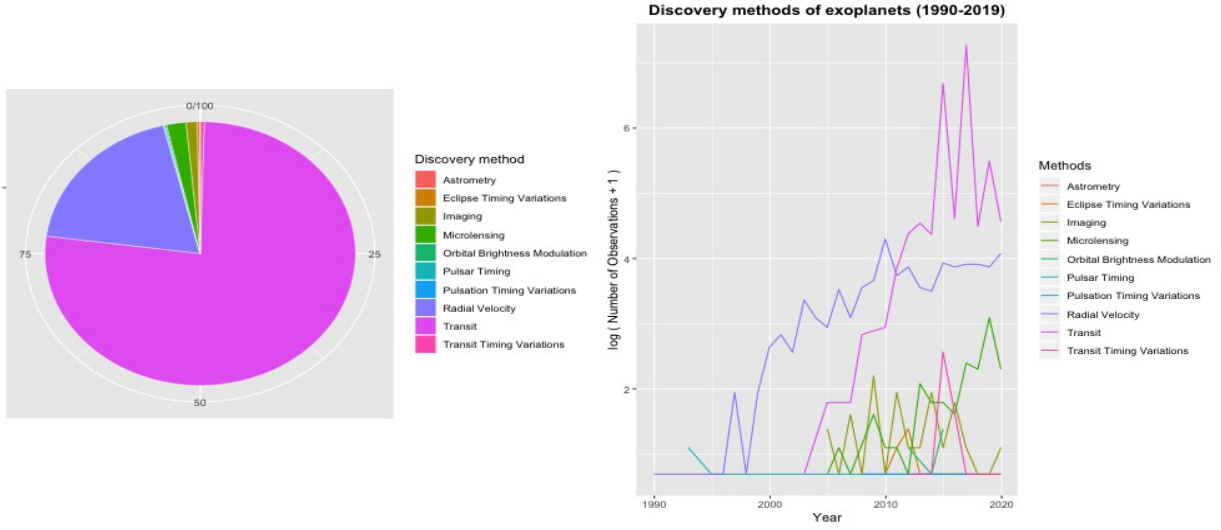


Figure 19: Discovery methods of exoplanets

Figure 20: Discovery methods of exoplanets over time

It is clear that the transit and radial velocity methods are the two most dominant methods currently used for exoplanet detection. Trailing those two methods are microlensing, followed by direct imaging. Curiously, astrometry seems to produce negligible results, despite the fact that it is taught as a major detection method in astronomy courses. We can see the progression of technologies via the line chart above, noting that the peak in exoplanet observations in 2017 can be attributed to the development of transit detection techniques.

One thing to mention is that typically when detection technology advances, one would expect a steady increase in results that levels off into a plateau. However, this is clearly not the case for both asteroid and exoplanet observations. The implication is that at each observational peak, we have already exhausted the pool of objects that we can find with the given technology. Afterall, there are only so many asteroids and exoplanets within our vicinity to be found. Thus, once we start noticing a decline in observations, we know that it is time for yet another technological upgrade in order to observe even farther than our previous capabilities.

4 Future Scope

This project was in no way exhaustive of the analyses that could be performed with the data we had acquired. In fact, there were many avenues that we wanted to pursue but could not due to computational limitations, a lack of expertise, time restraints, etc. In this chapter, we enumerate a few of the major ideas that we believe may be worth pursuing in the future.

4.1 Saturn's Rings

Based on the image of Saturn's rings (Figure 21), you can clearly see that there is a variation as you move along the axis. Saturn's rings are made of dust, grains, ices, etc. that have gathered and formed a structure due to Saturn's gravitational pull. We believe that there may be a similar gathering of asteroids around the Sun due to the Sun's gravitational pull. Treating the particles that make up Saturn's rings as miniature asteroids, we can compare the density distributions of asteroids around the Sun and particles around Saturn to see if any structural patterns can be identified.

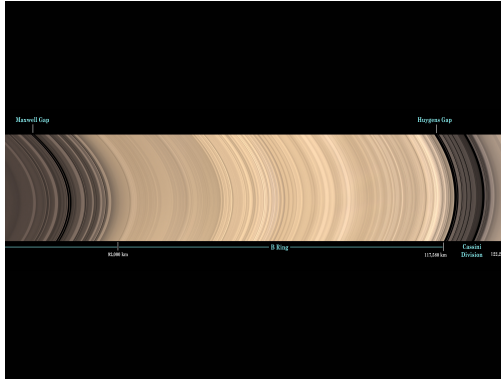


Figure 21: Saturn’s Rings

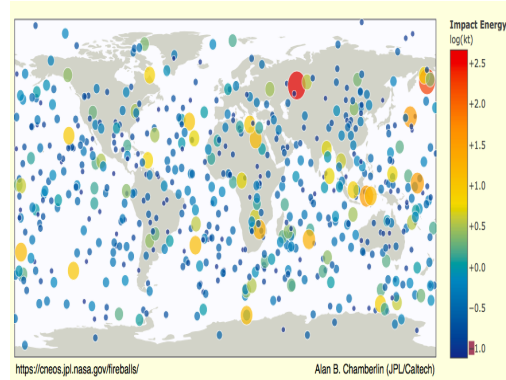


Figure 22: Fireballs reported by US government sensors

4.2 Future Impacts

Figure 22 shows a world map with meteor impacts across the globe that have happened in the past. Using orbital parameters provided in our datasets, we can calculate and trace out the orbits of PHAs in space, then compare their positions relative to Earth at given times in the future to create a similar ”Fireball” map for future impacts. Further factoring in an asteroid’s mass and velocity to predict its energy upon impact, a future impact map would be instrumental in formulating timelines for technological advancements related to asteroid impact preventative measures.

4.3 Exoplanet Discoveries

Mapping out exoplanet orbits from data gathered using different discovery methods may produce systematic differences that can be characterized. Knowing how specific discovery methods might bias results is invaluable in tweaking methods to account for accurate results. Furthermore, additional comparisons between data gathered from different methods can shed light onto which discovery methods are better or worse for specific types of planets and parent stars. Figure 23 shows the orbits of exoplanets in the Kepler-47 system.

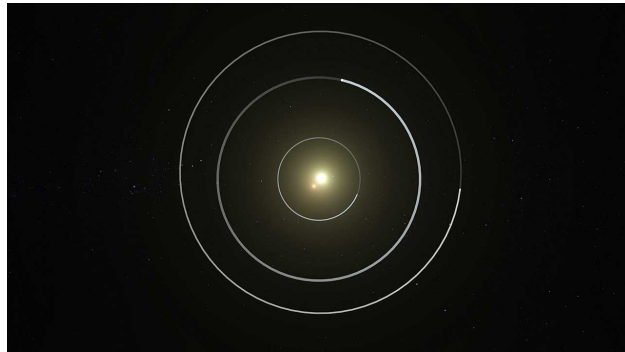


Figure 23: Orbit of exoplanets in the Kepler-47 system

5 References

- https://ssd.jpl.nasa.gov/sbdb_query.cgi#x
- https://exoplanetarchive.ipac.caltech.edu/cgi-bin/TblView/nph-tblView?app=ExoTbls&config=compositepars&fbclid=IwAR17XU2JPWDKpG1XCq6993J14alSN5r1W9zDIn-_D8lG2GRigqW_vS9nsmw
- <http://www.minorplanetcenter.org/iau/lists/Atens.html>

- <http://www.minorplanetcenter.org/iau/lists/Apollos.html>
- <http://www.minorplanetcenter.org/iau/lists/Amors.html>
- <https://space-facts.com/wp-content/uploads/asteroid-belt.png>
- <https://www.universetoday.com/wp-content/uploads/2014/10/Asteroid-classes-Apollo-aten.jpg>
- "Earth-Approaching Asteroids as Targets for Exploration," E. Shoemaker and E. Helin; in Asteroids: A Exploration Assessment, pp. 245-256.
- https://en.wikipedia.org/wiki/Potentially_hazardous_object
- <https://www.eso.org/public/images/eso0722e/>
- https://www.esa.int/ESA_Multimedia/Images/2019/02/Detecting_exoplanets_with_astrometry
- <https://teara.govt.nz/en/diagram/8008/gravitational-microlensing>
- <https://www.planetary.org/explore/space-topics/exoplanets/transit-photometry.html>
- <https://www.universetoday.com/140341/what-is-direct-imaging/>
- <https://cneos.jpl.nasa.gov/fireballs/>
- https://www.nasa.gov/sites/default/files-thumbnails/image/pia11142_cropped.jpg
- <https://www.skyandtelescope.com/astronomy-news/third-planet-found-orbiting-binary-star-system/>